# Chapter 5
# Numerical Investigation of Indoor Airflow and Particle Concentration

## 5.1 Introduction

The fundamental function of a ventilation system in a building is to maintain a healthy and comfortable indoor air environment with acceptable energy consumption. Two major concerns in ventilation system design, operation and malfunction diagnosis have been identified: (i) indoor air quality (IAQ) and thermal comfort, (ii) energy consumption and efficiency.

The issue of IAQ is gaining interest as it has significant influences on the occupants' health. People spend most of their time in indoor environments such as residences, offices, schools, workshops, etc. In Australia, more than 90% of the workforce works in an indoor environment and more than 50% of the workforce is employed in office environments (Jamiriska et al., 2003). The presence of contaminant particles may cause discomfort to the eyes, irritation of the respiratory system, and may even spread disease (Holmberg and Chen, 2003). In addition, an unhealthy indoor environment may decrease employees' productivity. It is estimated that lost productivity in the USA is nearly five times than that of direct medical costs (DTIR, 1995). To keep the indoor air healthy and clean, it is necessary to maintain a sufficient air exchange rate (ASHRAE, 2001). Here, the energy consumption and efficiency need to be taken into consideration. In modern society, energy consumption is increasing in buildings and it is predicted that this escalating trend may continue (OECD, 2003). In developed countries, it is estimated that 30~40% of energy is consumed in buildings and between 10% and 60% of this is used for air-conditioning and ventilation (Ellis and Mathews, 2002). For instance, ventilation and air-conditioning account for about 43% of energy consumed in commercial buildings in Australia (Langston, 1997)

To maintain a healthy IAQ and low energy consumption, the detailed information of indoor airflow and particles' concentration is essential for engineers' and scientists' study.

Several approaches have been employed to study indoor airflows and the motion of particles: experimental investigation, the zonal model and CFD. The experimental approach provides reliable information but it is rather expensive and impractical as a design tool. The zonal model approach gives a quick approximation of the overall flow but fails to provide the required detailed information. With increasing computational resources and the widespread availability of commercial code, CFD techniques are gaining in popularity and being used to predict indoor airflows and contaminant concentration. CFD has the capacity to provide "microscopic" information on the indoor air environment, like the air velocity, pressure, temperature and pollutants' concentration distribution which are useful to derive the relevant "macroscopic" parameters for engineering purposes (Chow, 1996). Furthermore, CFD produces the graphical presentation of the building configuration, velocity, pressure and contaminant concentration fields (Chow, 1996). Coupled with other building design tools such as Energy Simulation (ES), CFD helps engineers to modify the design towards achieving an optimal solution (Zhai and Chen, 2005)

There are basically two categories of computational approaches that are currently used to predict the gas-particle flows: the Eulerian-Eulerian model and the Eulerian-Lagrangian model. In the Eulerian-Eulerian model, both the gas and particle flows are treated as continuous fluid flow and regarded as interacting with each other. It is also found that in most of the CFD studies of indoor air-particle flows, the drift-flux multiphase model, which is in the framework of Eulerian-Eulerian approach, has been used rather than the fully coupled Eulerian model (Holmberg and Li, 1998). Murakami et al. (1992) studied the diffusion characteristics of airborne particles in a conventional flow-type clean room via the drift-flux model and the standard k-ε model. Validations against the measurements showed that the drift-flux model reasonably reproduced the concentration distribution of small airborne particles. By employing the drift-flux model and a Low-Reynolds-Number k-ε model, Chen et al. (1992) investigated the influence of location of airborne particle source, ventilation rate, air inlet size, air velocity, air outlet location, and heat source on the particle concentration distribution. They found that the particle concentration distributions in the recirculating zone are very sensitive to the location of the particle resource and airflow patterns. Shimada et al. (1996) studied the transport and dispersion of contaminant particles in a ventilated room via the standard k-ε model and the drift-flux model. From their calculations the concentrations were found to be in qualitative agreement with the measured results except in regions near the room floor and the walls. Holmberg and Li

(1998) also utilised the standard $k$-$\varepsilon$ model and the drift-flux model to simulate the particle transportation for indoor environment. It is shown that the particle deposition on indoor surfaces in an indoor environment plays a significant role towards the total pollutant balance even in the presence of low or no ventilation flow rate.

For the Eulerian-Lagrangian approach, the gas phase is solved by Eulerian equations and was then integrated with the Lagrangian equations for particle motion thereby tracking individual particle through the flow field. Chung (1999) investigated the air movement and contaminant transport in a partitioned enclosure provided with ventilation using the standard k-ε and Lagrangian particle-tracking model. The computed results of temperature and velocity fields agreed well with the measured data. The results also show that the predicted data of contaminant particle's trajectories gave valuable information to better evaluate the indoor air quality design procedure. Lu et al. (1996) simulated the air movement and aerosol particle deposition and distribution in a ventilated two-zone chamber consisting of a small opening between two compartments. Satisfactory agreement of the average particle concentrations between the Lagrangian predictions and measurements were obtained in both the zones. Buchanan and Dunn-Rankin (1998) investigated the particle transport characteristics in a hospital operating room using two of the commonly available cross-flow and impinging-flow ventilation configurations. From the analysis they concluded that numerical simulations can be a valuable design tool to control the transport of airborne contaminant particles. Recently, Zhao et al. (2003) numerically studied the air movement, aerosol particle concentration and its deposition in a displacing and mixing ventilation room using the Lagrangian model.

Despite the many encouraging results, some uncertainties still prevail in particular the approximation of turbulence models that requires further resolution (Chen, 1997). The indoor air flows are always characterized by low-Reynolds-number turbulence. The improper handling of LRN turbulence can contribute to inaccurate calculations of the airflows and consequently the contaminant concentration, since the particle dispersion and distribution are strongly affected by the air phase velocity and turbulent fluctuations. There are three techniques currently available to numerically solve the turbulence flow, which is the dominant flow pattern in indoor airflow: DNS, RANS and LES. DNS directly solves the Navier-Stokes equations of the gas phase. It provides the most accurate solutions. However, extremely fine meshes is required to solve the smallest eddies that are within the

size of 0.1 to 1 mm in an indoor flow (Spengler, 2001). Hence, the DNS approach is impossibly expensive in view of the computational standing for engineering flow and is only useful as a basic research tool for flows with low Reynolds number and simple geometry.

In the RANS approach for modeling turbulence, an approximation is introduced that all the flow unsteadiness is averaged out and the nonlinearity of the Navier-Stokes equations gives rise to terms that must be modeled. Although RANS model probably is the least accurate, it is quick, simple and possesses good numerical stability. When the model is properly applied, it provides reasonable results. The two-equation k-ε model is the most popular and used RANS turbulence model for the prediction of room air movement (Sorensen and Nielsen, 2003). It is easy to program and modify whilst giving reasonable results in many applications (Chen, 1997).

In contrast to RANS, LES takes advantage of the fact that larger eddies transport most of the momentum or thermal energy. In LES, large eddies are solved directly and the small eddies are modeled by the subgrid-scale (SGS) model, so it requires much less computing expense than DNS and it provides better results than RANS models in many cases. A SGS model based on the RNG theory has also been formulated through Yakhot et al. (1989). This RNG-based LES model is able to provide description of the low-Reynolds-number and near wall flow that are always encountered in indoor air flows.

LES is being increasingly employed as a tool to study turbulent flow for configurations in which RANS equations are not sufficiently accurate. Davidson and Nielsen (1996) employed Smagorinsky SGS LES model and a dynamic SGS model to simulate the flow in a three-dimensional ventilated room. They found that results of the dynamic SGS model were in good agreement with experimental data while Smagorinsky model gave poor performance. Emmerith and McGrattan (1998) utilized Smagorinsky SGS model to the ventilation airflow in a three-dimensional room. Their results were in good agreement with both experimental data and the LES results of Davidson and Nielsen (1996) except for the region near the floor and ceiling. Interaction between Smagorinsky constant and grid resolution was also reported. Zhang and Chen (2000) have applied a dynamic SGS model to calculate natural, forced and mixed convection air flows in enclosures. They have obtained reasonable agreement between the calculated air velocity, temperature and

turbulence distribution and corresponding experimental data. Recently, Jiang et al. (2003) used LES models to study the nature ventilation in buildings and found good agreement between the numerical results and experimental data. Kato et al. (2003) further employed the LES model to analyze the visitation frequency through particle tracking method and their simulation results were validated against a model experiment. Nevertheless, the in-depth investigations of the prediction of the indoor contaminant particle dispersion and concentration distribution using LES model are lacking.

The indoor airflow and contaminant particle concentration in two geometrically different rooms were investigated using the Eulerian-Lagrangian model in this chapter. For the first room configuration, the performances of three turbulence models, standard k-ε, RNG k-ε and the RNG-based LES model, for simulating indoor airflow were evaluated. The measured air phase velocity data obtained by Posner et al. (2003) were used to validate the simulation results. In the other two-zone ventilated room configuration (Lu et al. 1996), contaminant particle dispersion and distribution within the room were simulated using the RNG-bade LES model together with a Lagrangian particle tracking model. Corresponding experimental data of particle concentration decay from (Lu et al. 1996) were used to validate the simulation results. Several factors that may lead to the discrepancy between the CFD predicted results and the measured particle concentration were investigated and analysed.

## 5.2 Numerical procedure

The generic CFD code, FLUENT, is utilized to predict the air and particle flows under unsteady-state conditions. The Lagrangian particle tracking model is used to predict contaminant particle dispersion and concentration. Two-way coupling between the air and particle phases is achieved through the momentum exchange that appears as a sink term in the air phase momentum equations.

The transport equations are discretised using the finite-volume method. The time-dependent terms are handled through an implicit second order backward differencing in time. The QUICK scheme was used to approximate the convective terms at the faces of the control volumes for k-ε models. LES model is sensitive to the spatial disretization errors

because eddies near the cut-off wave-number is still energetic (Park et al., 2004). It has been reported that the truncation error overwhelms the contribution of SGS force for Upwind and Upwind-biased schemes (Mittal and Moin, 1997). So the central differencing scheme was used for LES model. The SIMPLE algorithm is employed as the pressure-velocity coupling method. This study employed an enhanced wall treatment which is a near-wall modeling method combining a two-layer model with enhanced wall functions. For LES model, if the wall layer is resolved, very fine mesh scheme is required. That is too computationally expensive for engineering applications. So, a wall model is adopted to reduce the computational expense, as described in FLUENT (2003).

The convergence criteria for the air phase properties (resolved velocities and pressure) are $10^{-5}$. The CFD code FLUENT normally has the default convergence criteria set at $10^{-3}$. The convergence of the solution is assumed when the residual is below the default convergence criteria (Sorensen and Nielsen, 2003). However, since the manner in which the non-linear equations reach the final solution is strongly problem dependent, the default convergence criteria may not ensure the numerical simulation is close to the final solution (Sorensen and Nielsen, 2003). The sufficiency of the convergence criteria is further checked by comparing the LES simulation of airflows in room 1 with the convergence criteria values of $10^{-5}$ and $10^{-7}$. The difference of air velocity profile between the two simulations is negligible.

## 5.3 Numerical results for the first room

Figure 5.1 illustrates the geometrical structure of room 1. The geometry has a floor area of 91.4 cm × 45.7 cm with a height of 30.5 cm. A partition with a height of 15 cm is located in the middle of the room. The inlet has the same size as the outlet, 10 cm × 10 cm. According to the experimental boundary condition (Posner et al., 2003), the inlet velocity ($U_{inlet}$) is 0.235 m/s with a uniform profile. Since the majority of the inlet air velocity profile is a laminar plug flow (Posner et al., 2003), the turbulent intensity is expected to be very low and assumed to be 1%. Based on the inlet velocity and the inlet width, the Reynolds number of the inlet airflow is determined to be 1500. The numerical simulations are obtained from a mesh density of 118 × 58 × 38 grids (structured mesh) for the whole domain. The grid-independency is achieved by refining the mesh to have a mesh density of

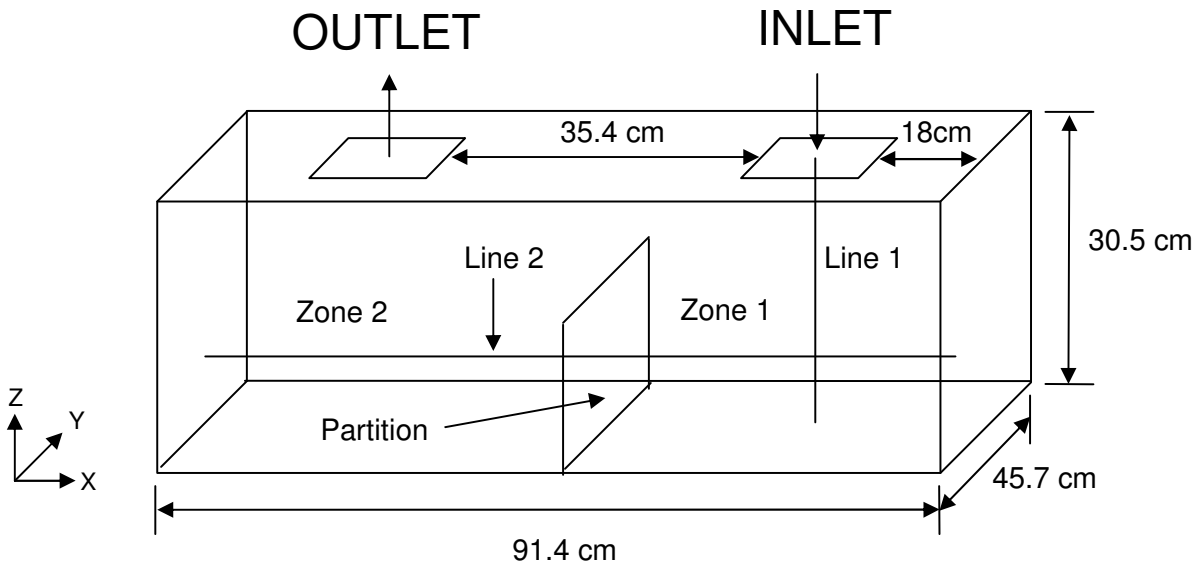


(a)

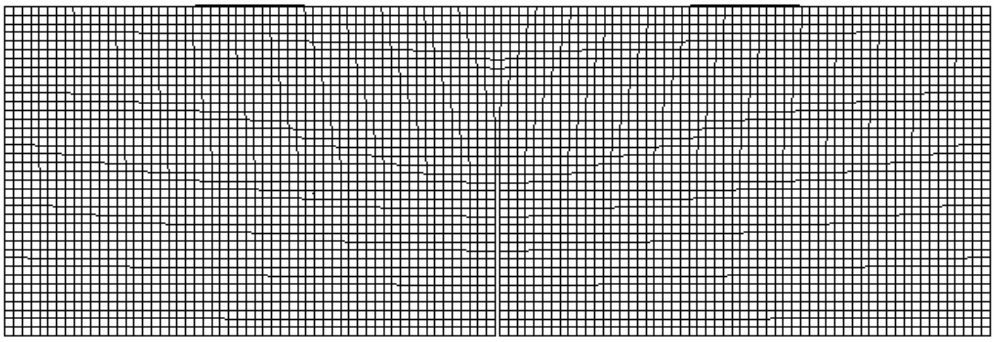

(b)

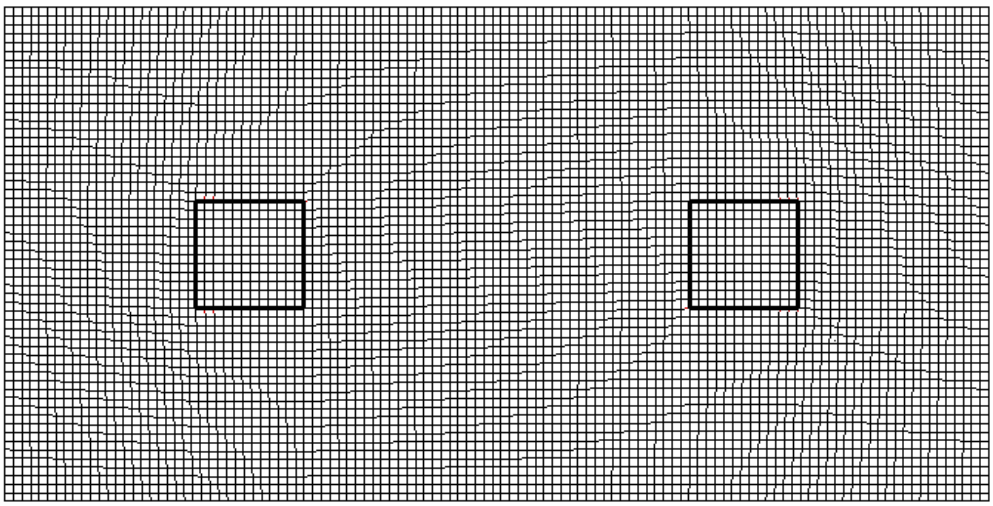

(c)

**Figure 5.1** (a) Configuration of room #1, (b) mesh for the mid-plane, (c) mesh for the room top

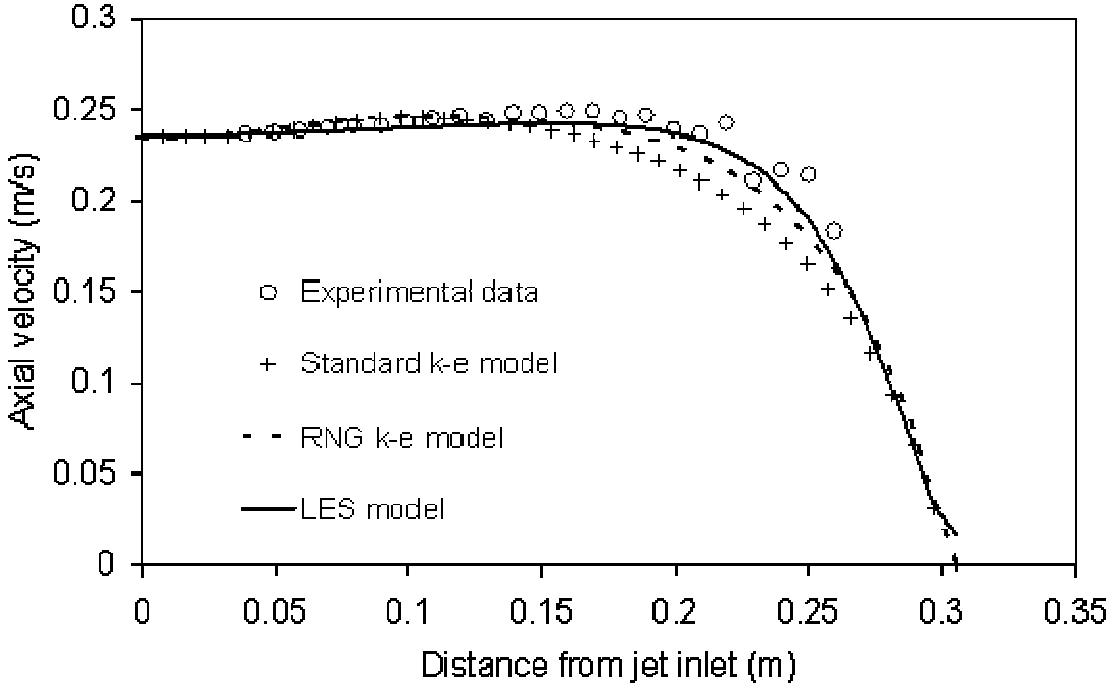


(a)

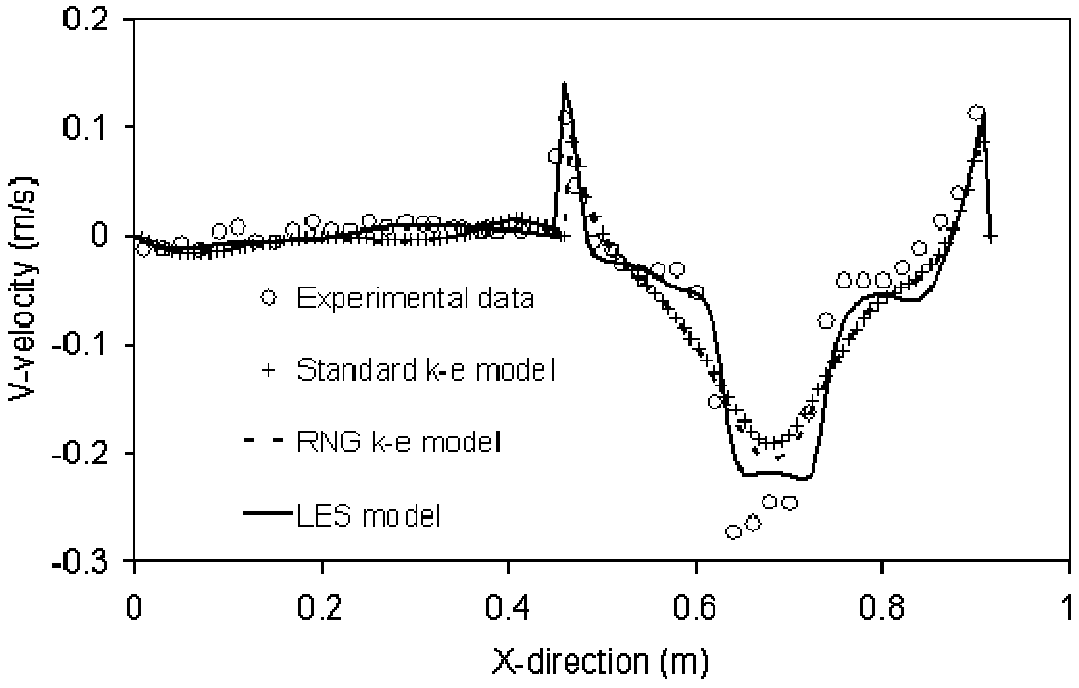


(b)

**Figure 5.2** Comparison between simulation and measured results of the vertical velocity component: (a) along the vertical inlet jet axis and (b) along the horizontal line at mid-partition height.

180 × 58 × 38 grids with the difference of the air phase velocity less than 1% predicted by RNG k-ε model. 12 × 12 grid points are allocated in the inlet and the outlet. The initial condition of the flow field in the room is assumed to be randomly perturbed about the mean velocity $U_{inlet}$. A non-dimensional time step of 0.0385 is used, which is defined by $t' = U_{inlet}\, t / H$ where $U_{inlet}$ is the inlet air velocity, $t$ is the physical time step (0.05 seconds) and $H$ is the room height. To ensure that the solution achieved sufficient statistical independence from the initial state, time-averaged results are obtained from the instantaneous values after the airflow simulation is marched for 2000 non-dimensional time steps, representing 100 seconds in physical time. After this time, the instantaneous values such as the airflow velocities are averaged over 10000 non-dimensional time steps, or 500 seconds in physical time. No visible difference is found between the time-averaged velocities when the simulation is continued after 500 seconds.

Figure 5.2(a) presents the comparison of the vertical air velocity along the vertical inlet jet axis (line 1 in Figure 5.1) predicted through the three turbulence models against the experimental data. Good agreement was achieved between all three turbulence model predictions and measurements. Nevertheless, the result from the RNG-based LES models provides the best agreement in the middle region from the distance of 0.15 m to 0.25 m. Herein, the velocities determined through the present standard k-ε model simulations were slightly under-predicted from those of RNG k-ε model, which were consistent with the computer investigations performed by Posner et al.(2003).

In the previous study of particle-gas flow over a backward facing step (Chapter 4), the performance of standard k-ε model and RNG k-ε model were investigated and analysed. It is found that standard k-ε model generally over predicts the gas turbulence kinetic energy $k$ in the flow, which leads to a high turbulent viscosity $\nu_{g,t}$ defined as $\nu_{g,t} = C_\mu \frac{k_g^2}{\varepsilon_g}$. Figure 5.3(a) shows the predicted turbulent kinetic energy k normalised by 0.005 kg/ms along the vertical inlet jet axial (line 2 in Figure 5.1), and Figure 5.3(b) demonstrates the profile of the turbulent dissipation rate ε normalised by $0.01 m^2/s^3$. It is evidently clear that the standard k-ε model yielded excessive normalised turbulent kinetic energy values while the predicted normalised turbulent dissipation rate ε values at the same locations were almost the same as RNG k-ε model. This therefore resulted in the over prediction of $\nu_{g,t}$ and the

production of excessive mixing in the standard k-ε model, which reduced jet velocity. Another possible cause could be the ε transport equation of the standard k-ε model (discussed in Chapter 3). Figures 5.4(a) and (b) illustrate the turbulent viscosity profiles obtained by the standard k-ε and RNG k-ε models at the mid-plane of zone 1. It is evidently clearly that the standard k-ε model predicted higher turbulent viscosity values than those of the RNG k-ε model in the central region.

Figure 5.2(b) shows the comparison between the predicted and measured vertical air velocity component along the horizontal line at mid-partition height. From the location x = 0 m to the partition, all the three turbulence models yielded almost similar results, while RNG-base LES model gave slightly better prediction in the region from x = 0.2 m to the partition. In the near-wall regions about the locations x = 0.46 m and x = 0.9 m, the RNG-based LES model was seen to successfully captured the highest positive vertical velocities while k-ε models significantly under-predicted the velocities. From these results, it was clear that better prediction was achieved through the RNG-based LES model as demonstrated through the excellent agreement with the experimental results in the region from the partition to x = 0.6 m. Significant under-prediction of the negative vertical velocity by k-ε models, found in the region right beneath the inlet, could be attributed to the over-diffusion caused the eddy-viscosity modelling. Marginal discrepancy between the measured data and the simulation results could be found in the region about the location x = 0.85 m where k-ε models results were marginally better than the RNG-based data. Overall, all the three turbulence models performed well; good agreement has been achieved between the predictions and measured data and the flow trends have been successfully captured through the three turbulence models. One important finding in this investigation was that the RNG-based LES model has shown to provide significantly better results especially in zone 2 because the model better accommodated the flow behaviour within the model room.

Based on the parametric study performed above, there are three principle advantages that RNG-based LES model has demonstrated to perform better over the two-equation k-ε models. Firstly, RNG-based LES model explicitly solves the large eddies that transport the momentum energy and turbulence, and only models the small subgrid-scale eddies. As a result, RNG-based LES model is less sensitive to the modelling errors than the k-ε models

(see Figures 5.2(a) and (b)). Secondly, RNG-based LES is suited for LRN turbulent flows that are of importance for indoor airflows. It is well known that the Smagorinsky SGS LES model, which is based on high Reynolds number flow, predicts non-zero turbulence viscosity in laminar flows. RNG-based LES model remedies this problem by introducing a ramp function in Equation 3.32. In low turbulent flow regions (for instance the laminar flows), the argument of the ramp function becomes negative and the effective viscosity recovers the molecular viscosity. This enables the RNG-based SGS eddy viscosity to model the low-Reynolds-number effects encountered in transitional, laminar flows and near-wall regions that are always encountered in indoor airflows. Semi-empirical models such as the standard and RNG k-ε models tend to better handle high-Reynolds-number flows as their constants were tuned by the experimental data of fully developed turbulent flows. Thirdly, RNG-based LES captures the instantaneous turbulences, i.e. it can properly account for the history and transport effects on turbulence; the k-ε models are incapable because of the inherent time-averaging modelling approach. This can be clearly shown in Figure 6.5 that compares the statistic root-mean-square (RMS) velocity profiles in the room middle-plane obtained by three models. RNG-based LES model predicted significantly higher RMS velocities than the others, that coincides with the above analyse. With the injection of contaminant particle into the enclosed environment, it is anticipated that the RNG-based LES model is expected to provide better prediction of the contaminant particle dispersion and concentration distribution that are strongly affected by gas-phase flow and time-dependant.

The time-mean velocity fields simulated by the three turbulence models at the mid-plane of the model room are compared in Figure 5.6. All the three models successfully predicted the strong recirculation cell in the region about the location x = 0.85 m. k-ε models predicted larger recirculation zone than the RNG-based LES model indicating a larger dispersion of the airflow.

As mentioned previously, one of the advantages of the LES model is that it can account for the historical and the transport effects on turbulence, i.e. it captures the instantaneous turbulences. Figure 5.7(a) illustrates the instantaneous velocity profile at the mid plane. Four recirculation structures are seen in zone 1, which indicate the strong mixing of the air and particles there. However, these circles are not shown in the time-mean velocity profile

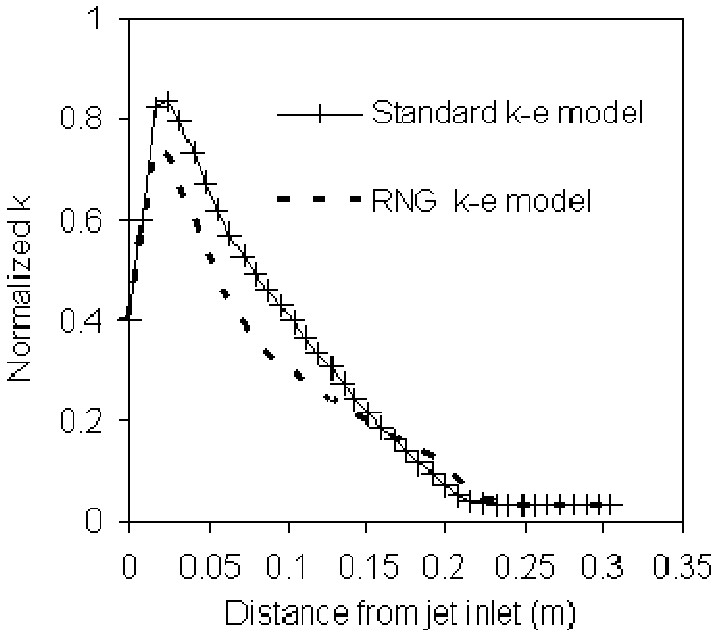


(a)

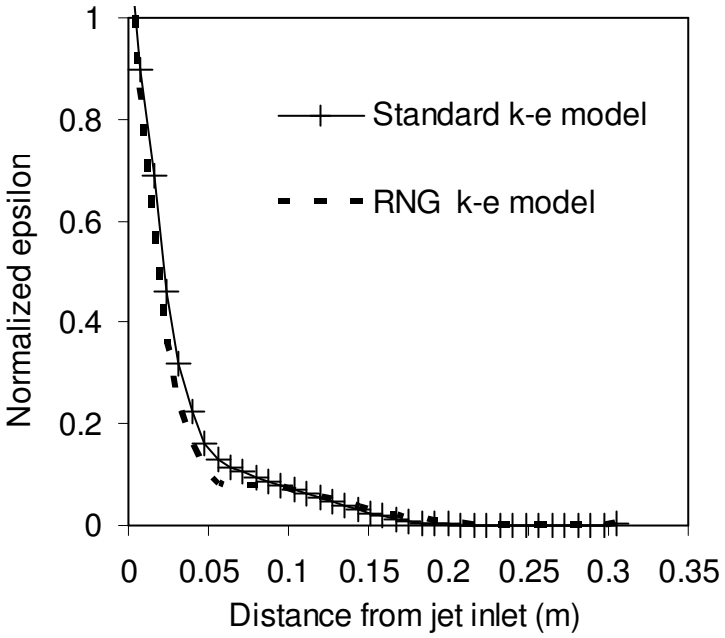


(b)

**Figure 5.3** (a) the computed turbulent kinetic energy k (normalized by 0.005 kg/ms) and (b) the computed turbulent dissipation rate ε (normalized by $0.01 m^2/s^3$) along the vertical inlet jet axis.

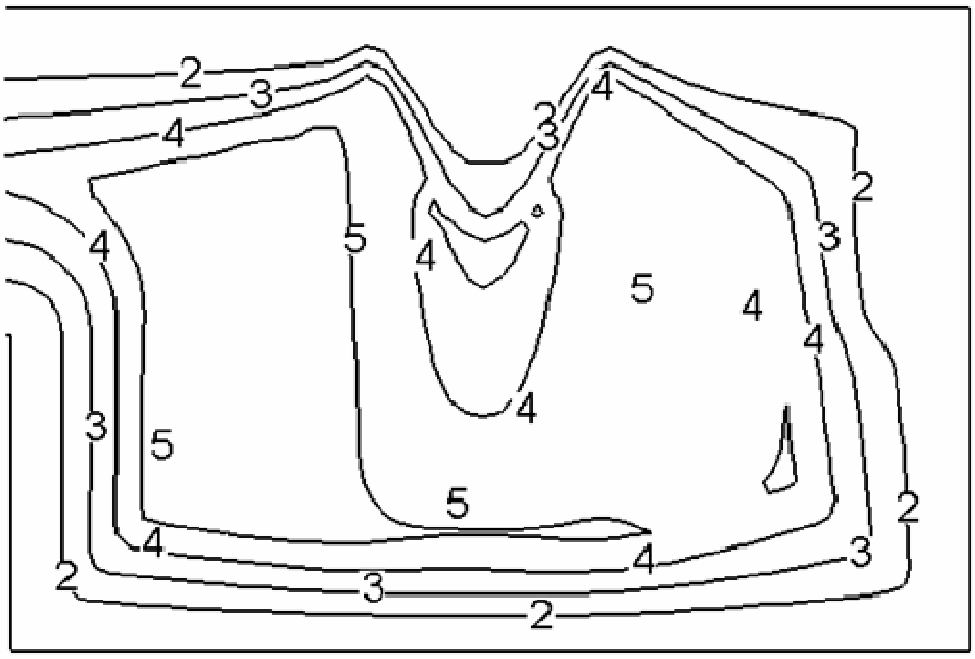


(a)

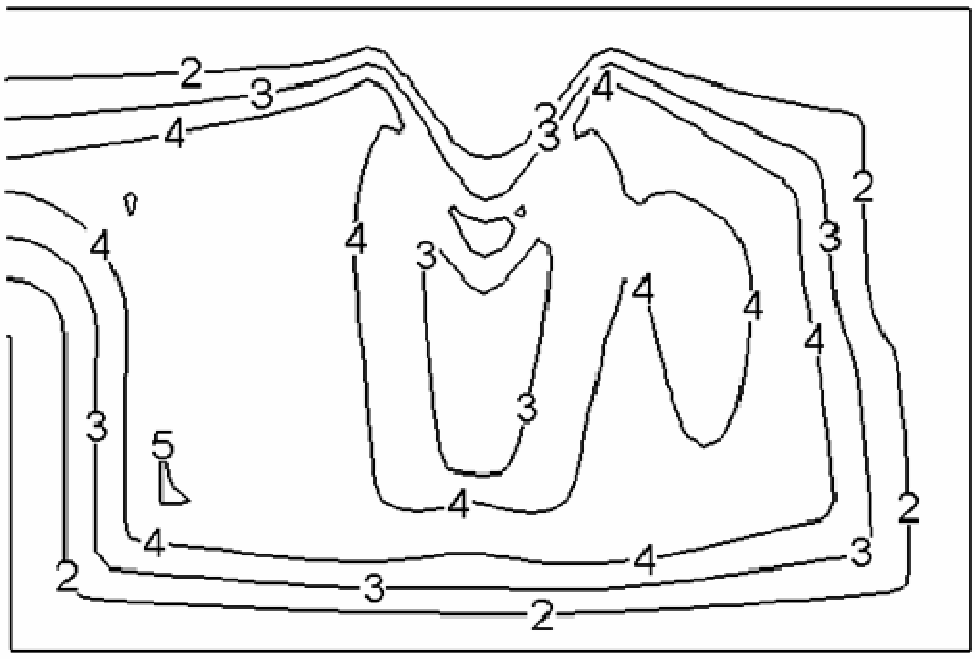


(b)

| Level | 1 | 2 | 3 | 4 | 5 |
|---|---|---|---|---|---|
| Turbulent viscosity (kg/ms) | 0.0002 | 0.0004 | 0.0006 | 0.0008 | 0.001 |

**Figure 5.4** The turbulent viscosity profiles predicted by (a) standard k-ε model and (b) RNG k-ε model.

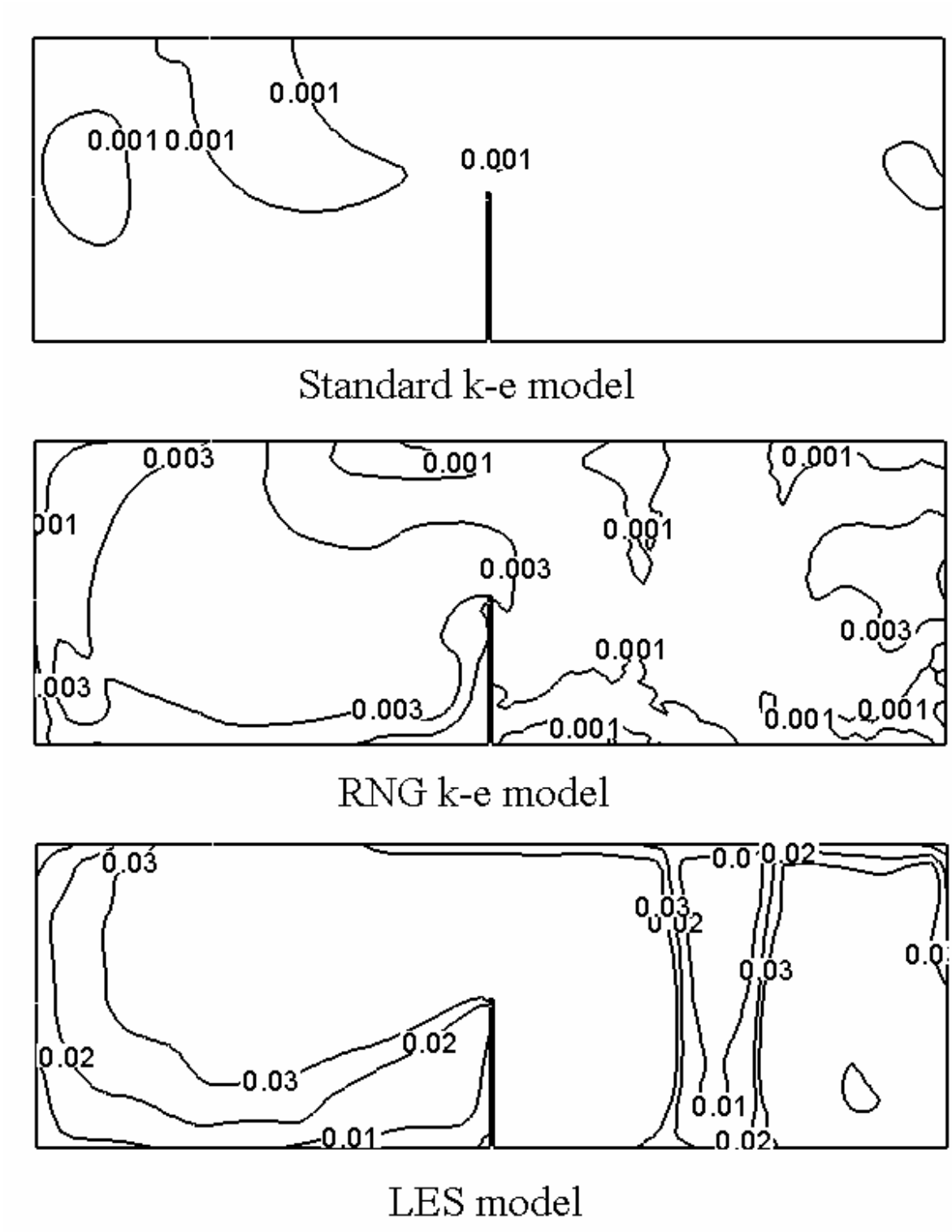


**Figure 5.5** Comparison of predicted RMS velocity in the mid-plane of the room.

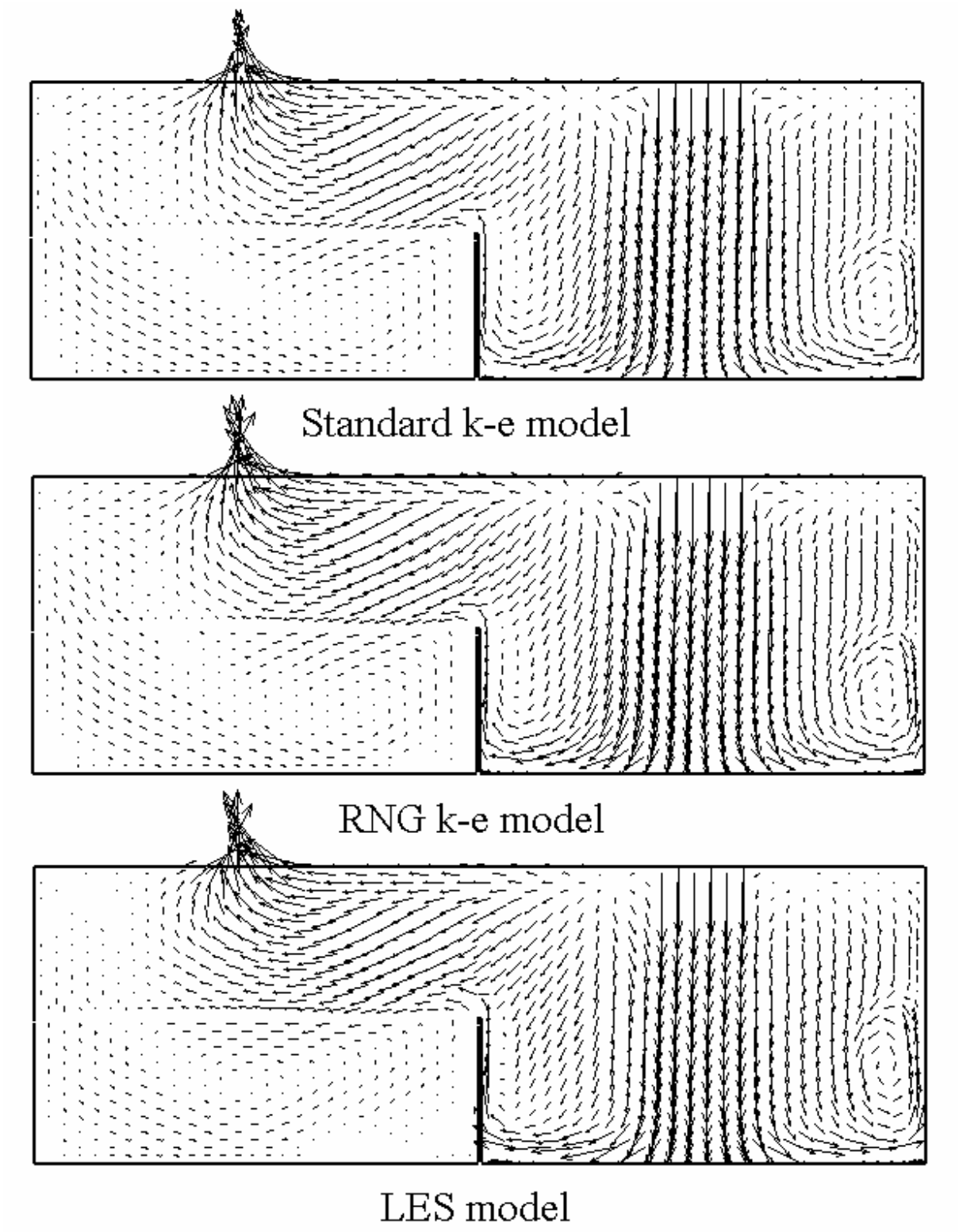


**Figure 5.6** Comparison of the predicted time-mean velocity field in the mid-plane of room 1.

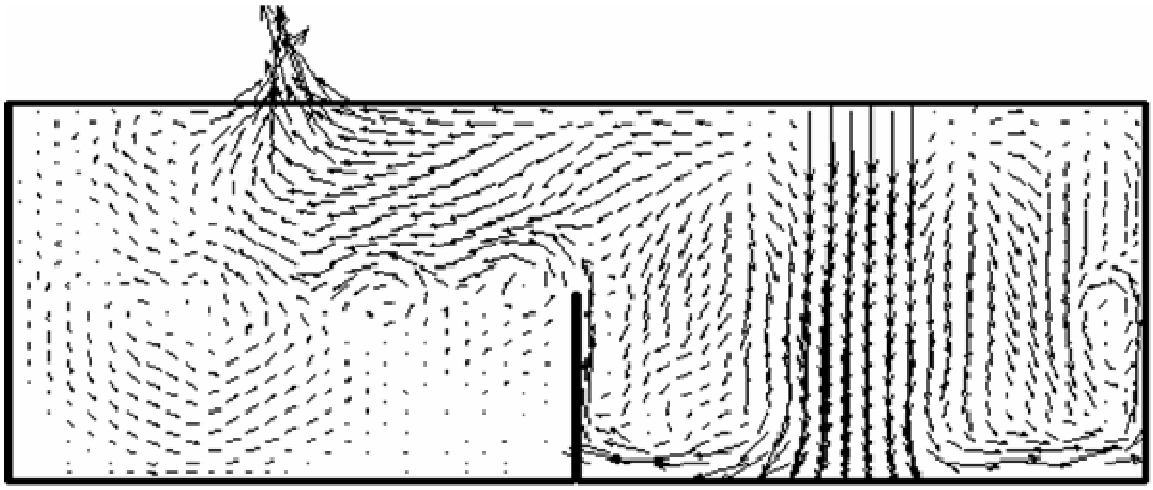

(a)

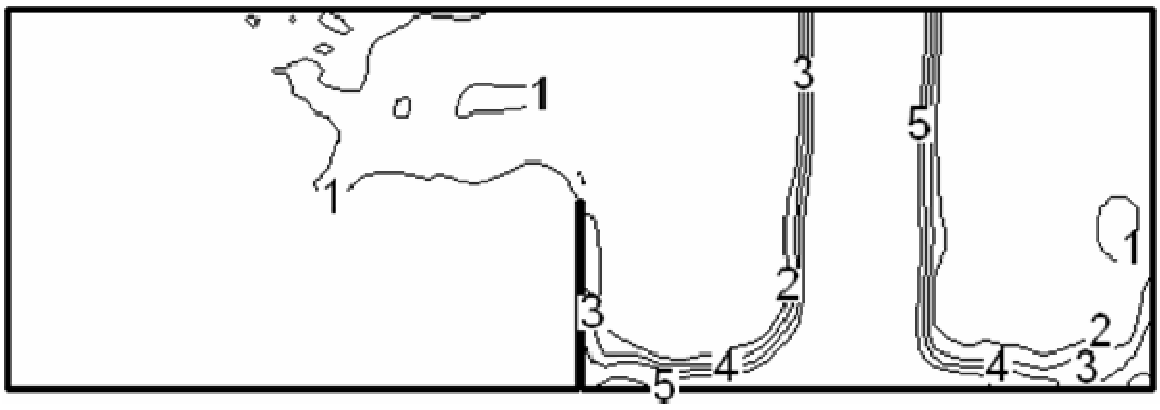


(b)

| Level | 1 | 2 | 3 | 4 | 5 |
|---|---|---|---|---|---|
| Total Pressure | 0.02 | 0.0095 | 0.017 | 0.0245 | 0.032 |

**Figure 5.7** LES prediction (a) instantaneous velocity field of the mid-plane, (b) instantaneous total pressure profile of the mid-plane.

in Figure 5.6. It is noted that the lack of instantaneous information may lead to inappropriate evaluation and design of the ventilation systems. This has been confirmed through the LES investigation of natural ventilation in a building with a large opening (Jiang et al., 2003). In that study, it was found that fresh-air streamlines reached the wall opposite to the opening in the instantaneous prediction. Nevertheless, the streamlines in the mean flow field presented a recirculation zone indicating that the fresh air could not have penetrated so profoundly into the enclosure. LES certainly thereby provides a way to account for the instantaneous information. The instantaneous total pressure profile along

the mid plane is given in Figure 5.7(b). Higher total pressure is found in the inlet jet region and the low pressure is seen in zone 1.

In indoor air-pollution problems, concerns are mainly focused on fine particles (aerodynamic diameter that is smaller than 2.5 μm), this study investigated the prediction of particle (with diameter of 1 μm having a density of 800 kg/m$^3$) concentration by the three turbulence models. From the elapsed time of 70 seconds, 144 particles, evenly-spaced, were injected at the inlet vent, with the same velocity as the inlet air, until the simulation time has reached 100 seconds. In total, there were 86400 particles introduced in the room until the elapsed time of 100 seconds. The particle injections were subsequently stopped, and only the sample particles remained in room were tracked until the time reached 160 seconds. Indoor airflows are always a feature with low characteristic velocities and the contaminant particles are with small diameters. So in most cases, the Stoke aumber for the contaminant particles flow indoor is far less than unity and the particles act like gas tracers.

Figure 5.8 presents the comparison of tracked sample particles numbers obtained from the different turbulence models for the particle size, $d_p$ = 1 μm. After an elapsed time of 85 seconds, the three turbulence models tracked almost the same number of contaminant particles. Here, the contaminant particles were just entering the room. Majority of the particles were concentrated in Zone 1 of the model room with very few particles flowing out through the outlet vent. At times $t$ = 100 seconds and $t$ = 115 seconds, the RNG-based LES model were seen to track more contaminant particles than the $k$-$\varepsilon$ models, i.e. more contaminant particles were predicted to be suspended in the room through the RNG-based LES model. Here, since the size of the particles were small ($St$ << 1), the particles acted like fluid traces thereby the prediction results of the gas phase velocity and turbulence strongly affected the contaminant particle dispersion. For the RNG-based LES model, the velocity fields were correctly calculated and the three-dimensional instantaneous turbulence was adequately simulated, which strongly influenced the particle phase resulting in more realistic particle dispersion than the $k$-$\varepsilon$ models. In Figure 5.9, the simulated contaminant particle concentrations at the mid-plane of the model room at time $t$ = 100 seconds were compared. The $k$-$\varepsilon$ models predicted higher concentration in the inlet jet region than the RNG-based LES model. In the regions next to the right side wall, the

RNG-based LES model predicted higher particle concentration. Also, in Zone 1 of the model room, where the air phase velocity was low, the RNG-based LES model simulated particles in higher concentration and wider regions than the *k-ε* models.

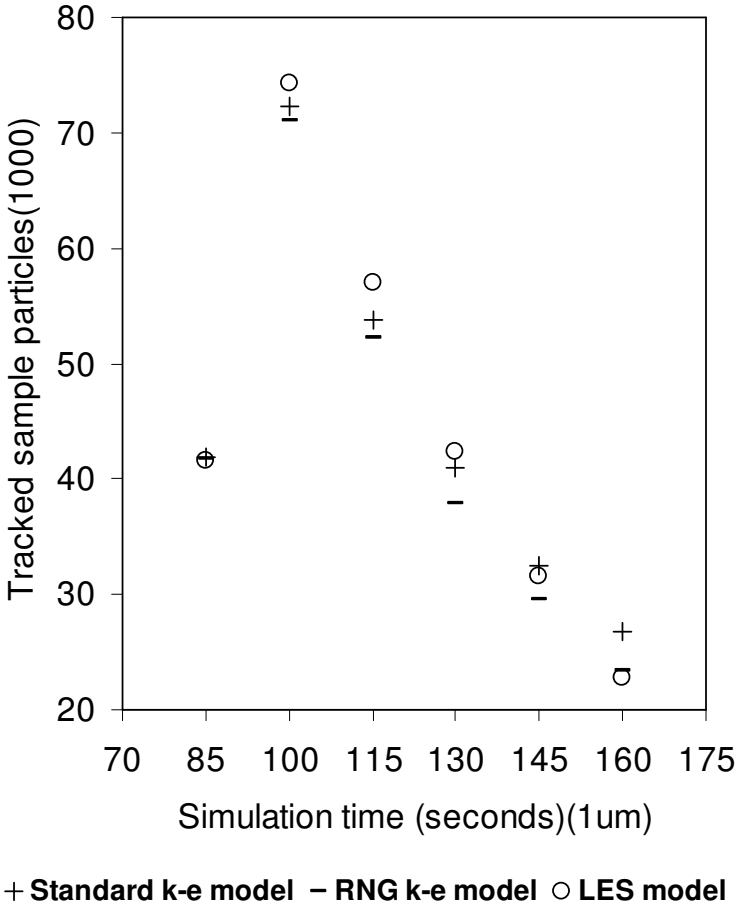


**Figure 5.8** Comparison of tracked sample small particles utilising the various turbulence models.

After an elapsed time of 100 seconds, the particle injection was stopped and particles in the room were dispersed with the air flow. In Figure 5.9, it has been shown that at time t = 130 seconds, the RNG-based LES model tracked marginally more particles than the standard k-ε model, while the RNG k-ε model tracked even less than the other two turbulence models. A closer investigation on the simulated particle concentration shown in Figure 5.10, at time t = 130 seconds, that for the simulations using the RNG-based LES model, as more particles had been dispersed into the left part of the room and the air velocity is very low, higher particle concentration can be found in the lower part of zone 2. At time t = 160 seconds, the RNG-based LES model tracked almost the same particle number as the RNG k-ε model. However, the standard k-ε model tracked even more particles than the other two models. Figure 5.11 shows the comparison of the contaminant particle concentration

simulated by the three turbulence models at the mid-lane of the model room at time t = 160 seconds. For RNG-based LES model, more particles in the lower left part of the room were dispersed to the upper left part and then flew out of the outlet.

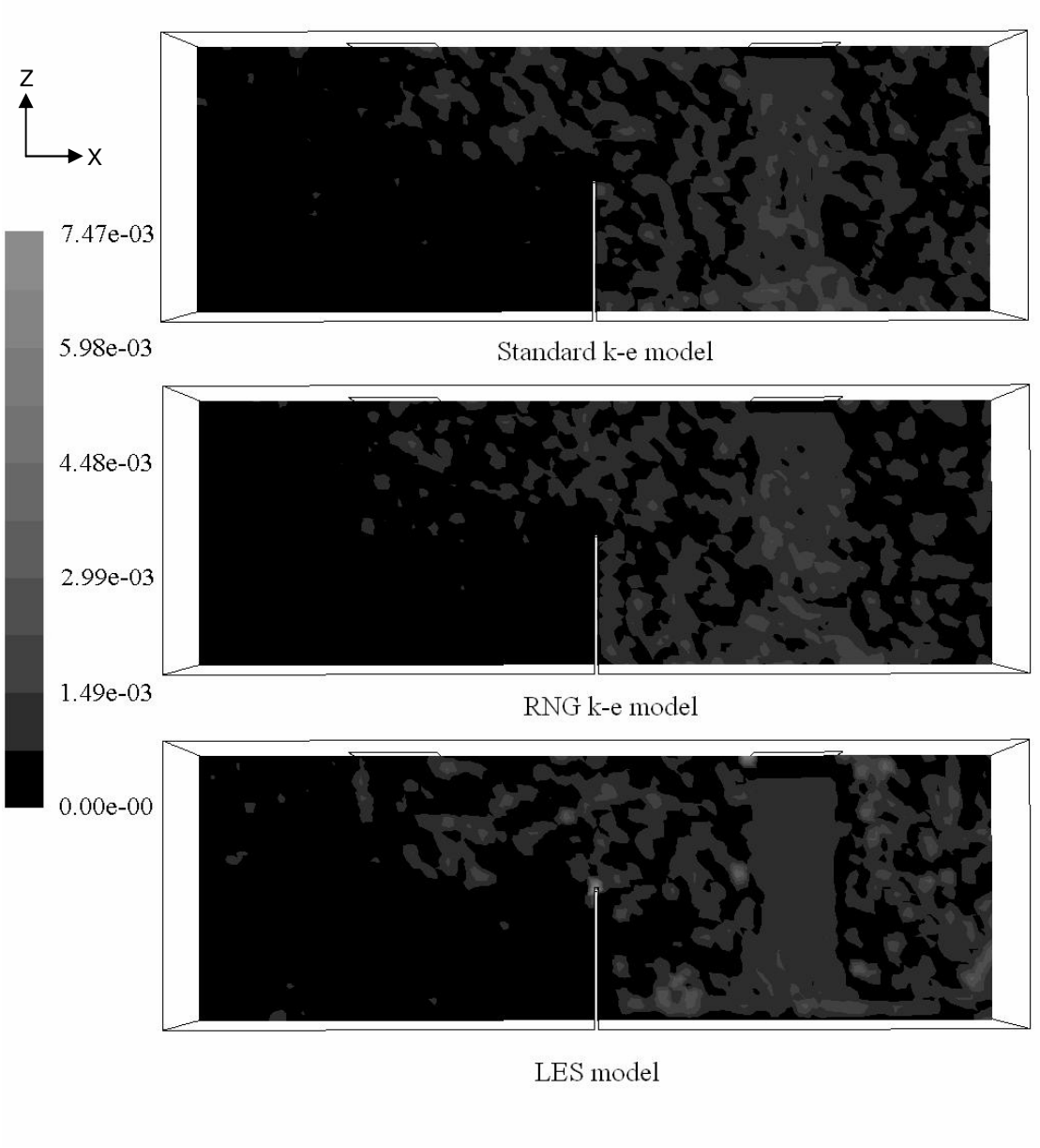


**Figure 5.9** The comparison of the contaminant particle concentration ($d_p$ = 1 μm) simulated by three turbulence models at the midplane of the model room after an elapsed time of 100 seconds.

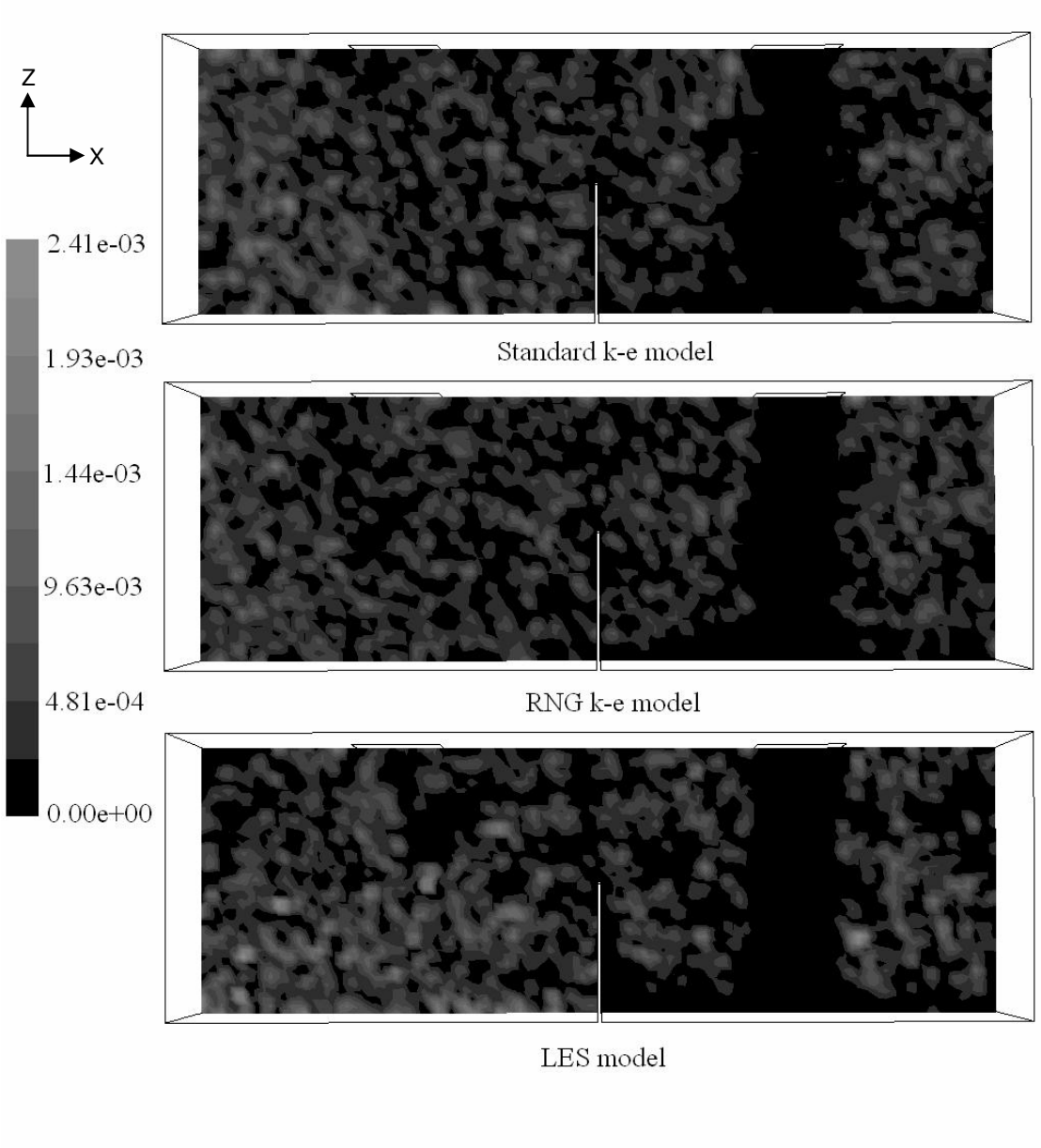


**Figure 5.10** The comparison of the contaminant particle concentration ($d_p$ = 1 μm) simulated by three turbulence models at the midplane of the model room after an elapsed time of 130 seconds.

For small particles, the discrete random walk (DRW) model used in this study may have a deficiency when the k-ε models are employed for the gas phase. In strongly inhomogeneous diffusion-dominated flows where small particles should become uniformly distributed, DRW combining with k-ε models may predict high concentration in low-turbulence region of the flow (MacInnes and Bracco, 1992). Nevertheless, no evidences of this unphysical phenomenon have been found in this study.

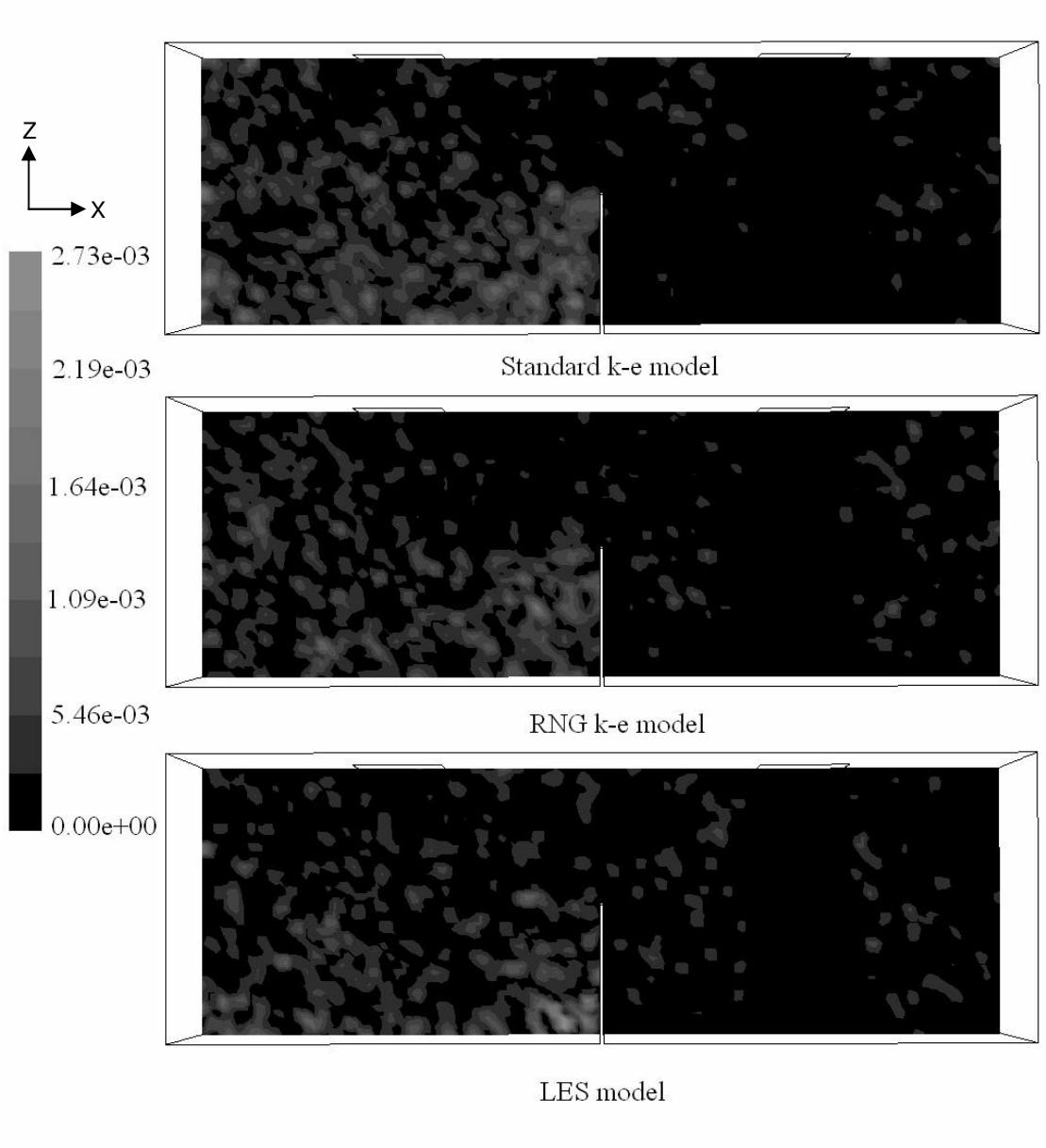


**Figure 5.11** The comparison of the contaminant particle concentration ($d_p$ = 1 μm) simulated by three turbulence models at the midplane of the model room after an elapsed time of 160 seconds.

Figure 5.12 presents the comparison of tracked sample particles numbers obtained from the different turbulence models for the particle size, $d_p$ = 10 μm. Here again, the three turbulence models tracked almost the same number of contaminant particles after an elapsed time of 85 seconds where the large particles were just entering the model room. At times t = 100 seconds and t = 115 seconds, the RNG-based LES model has demonstrated again to track more contaminant particles than the k-ε models. As time progressed, the k-ε models showed a significant drop in tacking the contaminant particles, i.e. less suspension

of contaminant particles in the air flow. It was notable herein again that the RNG k-ε model tracked fewer particles than the standard k-ε model.

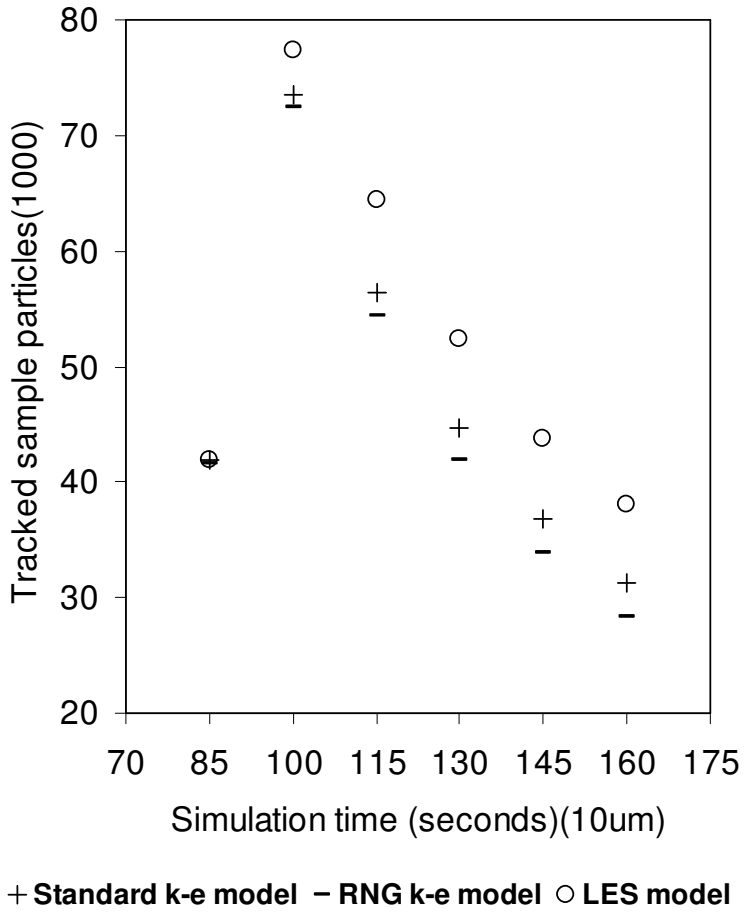


**Figure 5.12** Comparison of tracked sample large particles utilising the various turbulence models ($d_p$ = 10 μm).

## 5.4 Numerical results for the second room

The particle concentration decay within a two-zone ventilated room (Lu et al. 1996) is investigated using the RNG LES model with Lagrangian particle-tracking**.** Figure 5.13 shows the geometry configuration of this room with a size of width × depth × height = 5 m × 3 m × 2.4 m. In the middle of the room, a partition with a large opening of height and width of 0.95 m × 0.70 m divides the room into two zones. The inlet (with size of 1 m in y direction and 0.5 m in z direction) is 1.6 m above the room floor and 1.5 m from the front wall. An outlet with the same size as the inlet is 0.3 m above the floor and 0.5 m from the front wall. Two air exchange rates are tested in this study: (1) air change per hour (ACH) 10.26 with inlet velocity of 0.1026m/s; (2) air change per hour (ACH) 9.216 with inlet

velocity of 0.09216m/s. The grid independence is checked by comparing the computed particle concentration decay obtained by three different mesh densities of 50 × 30 × 24, 63 × 38 × 30 and 83 × 50 × 40 (all are structured meshes) for the 9.216 ACH. The difference between predicted particle concentration decay from the 63 × 38 × 30 and 83 × 50 × 40 mesh densities is negligible. The mesh density of 63 × 38 × 30 is used in this study in order to embrace the increase of computational efficiency towards achieving the final results.

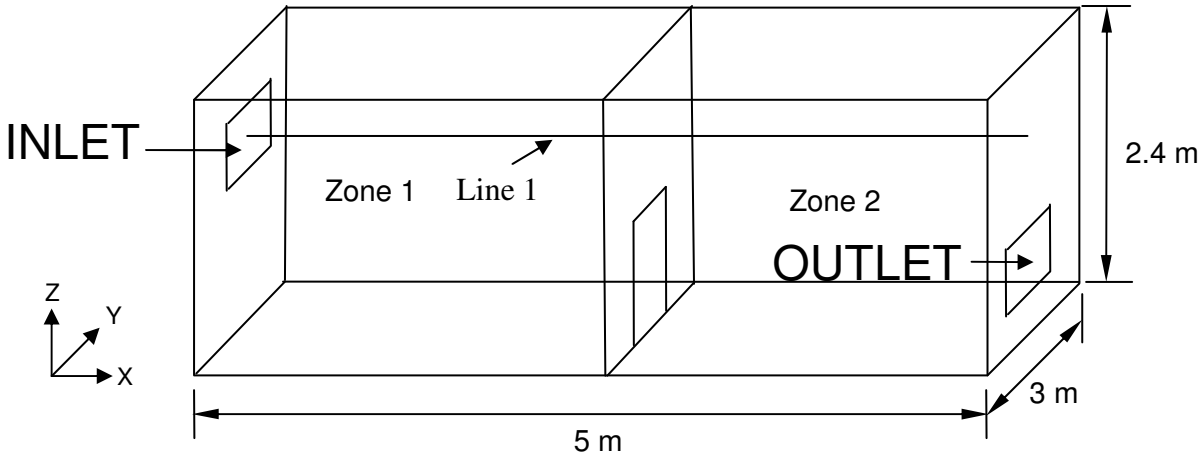


**Figure 5.13** Configuration of room 2.

Figure 5.14(a) presents the time-mean air phase velocity field at the mid-plane (y=1.5m) without injected particles for 10.26 ACH. The velocities are averaged over successive 30 minutes periods with the initial 5 minutes discarded. The non-dimensional time step is set at 0.005. The averaged y+ is about 4, which is acceptable as it is inside the viscous sublayer (y+ < 5) (FLUENT 2003). The time-mean static pressure along the mid-plane of room 2 is presented in Figure 5.14(b). Higher pressure can be found at the right upper corner in zone 1 where the air is forced to flow downwards along the wall. In the opening region where a positive pressure gradient exists, the static pressure drops rapidly. At the right lower corner in zone 2, a negative pressure gradient is found where the air is forced by wall to flow upwards. This study investigates the prediction of 8000 sample particles (having equal sizes ranging from 1 to 5 μm and a density of 865 kg/m$^3$). At the beginning of the simulation, the sample particles are released into the whole volume of zone 1 uniformly with zero initial velocity. The particle tracking period is 29 minutes for the case of 10.26 ACH, while 26 minutes for 9.216 ACH.

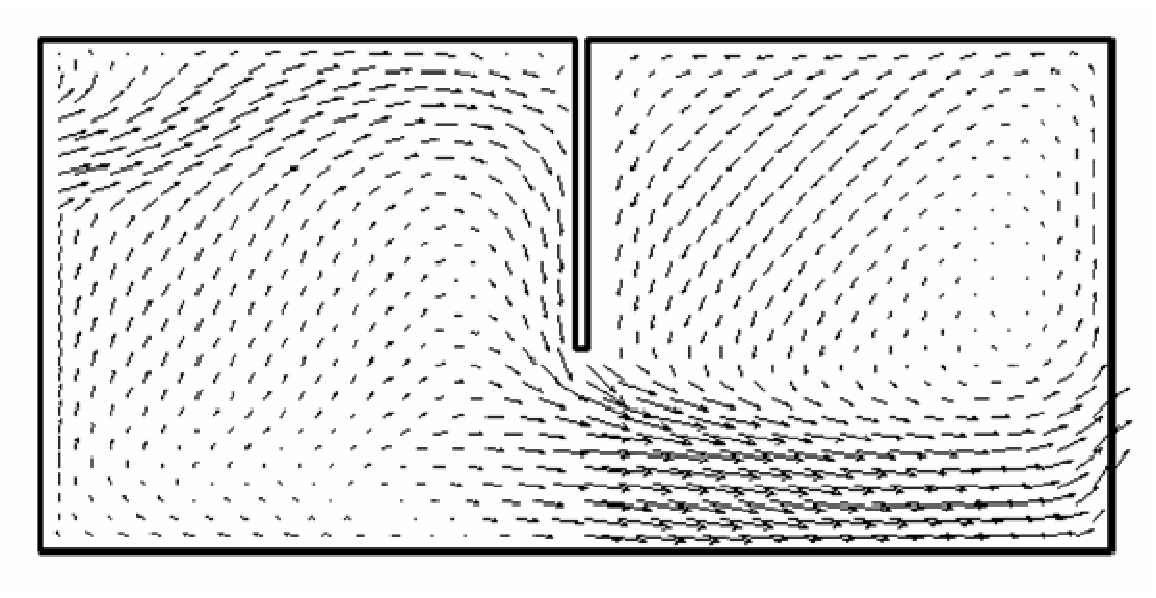

(a)

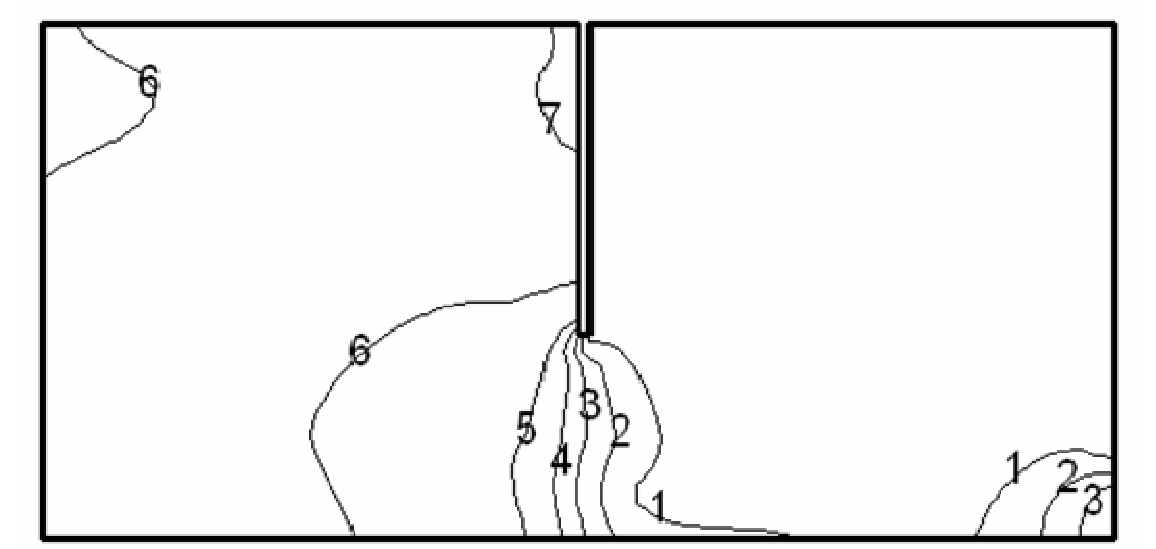


| Level | 1 | 2 | 3 | 4 | 5 | 6 | 7 |
|---|---|---|---|---|---|---|---|
| Pressure | -0.0085 | -0.007 | -0.0055 | -0.004 | -0.0025 | -0.001 | 0.0005 |

(b)

**Figure 5.14** (a) Predicted time-mean air velocity field of the mid-plane in room 2 and (b) Predicted time-mean static pressure of the mid-plane in room 2.

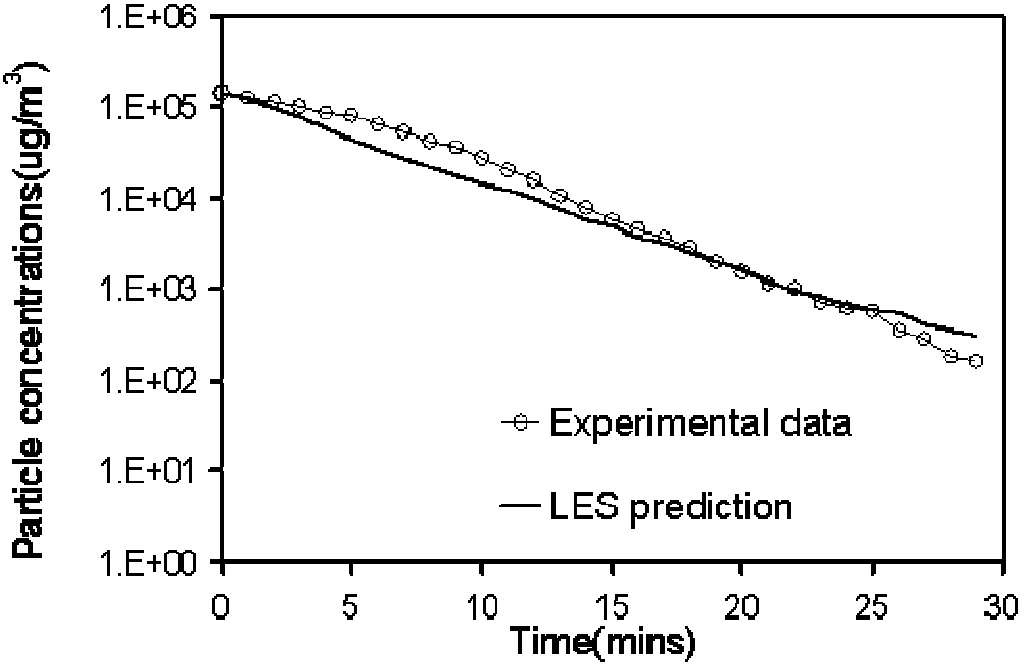


(a)

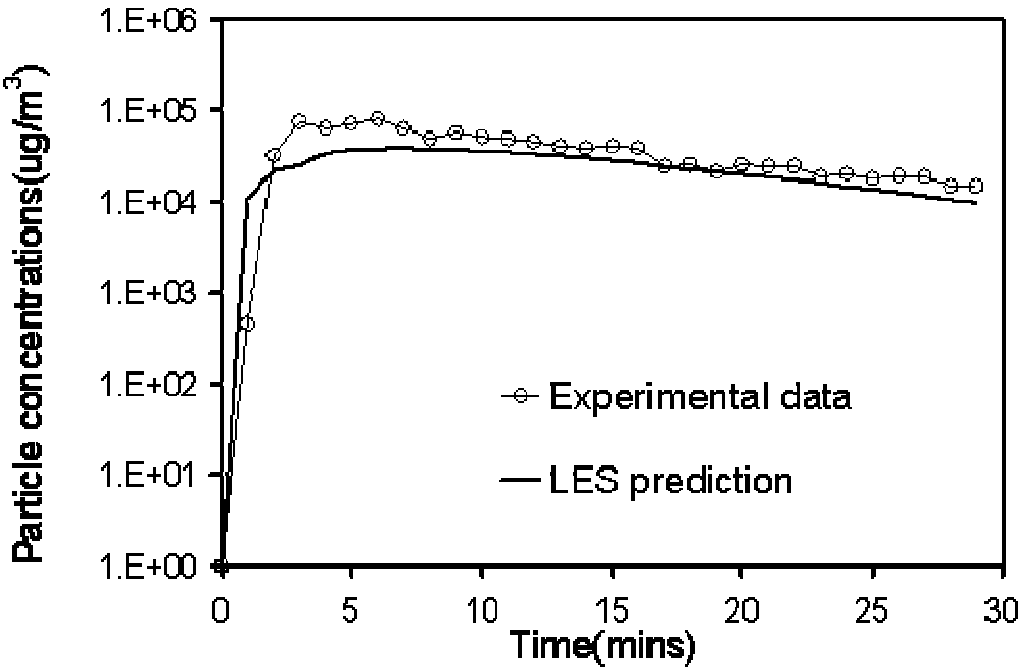


(b)

**Figure 5.15** The predicted and measured zone-averaged particle concentration decay ACH=10.26 1/H (a) zone 1 and (b) zone 2. (Particles depositing only on room floor)

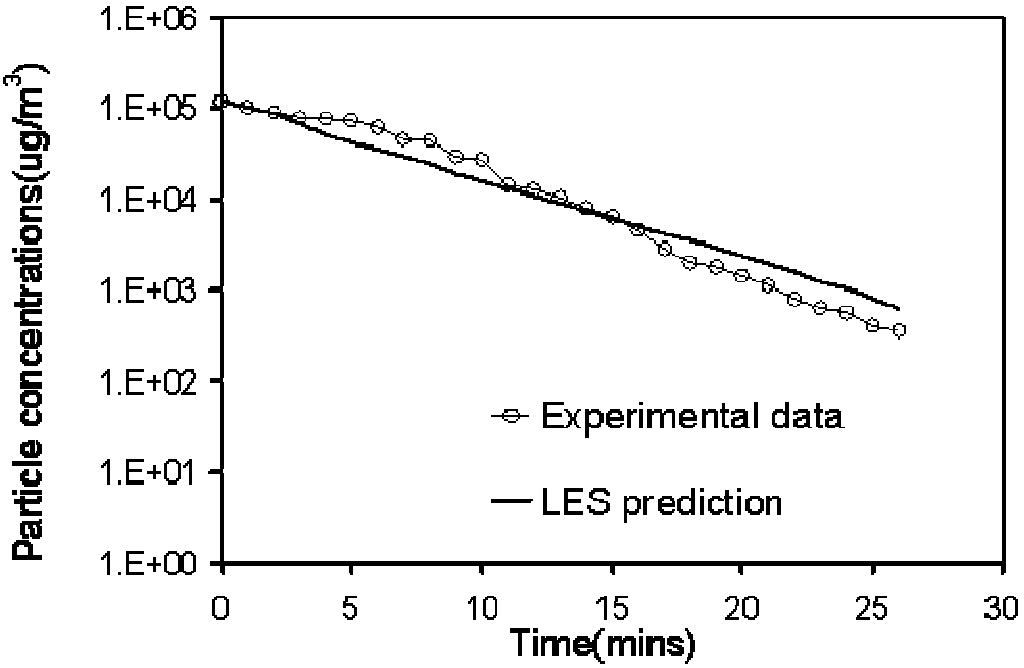


(a)

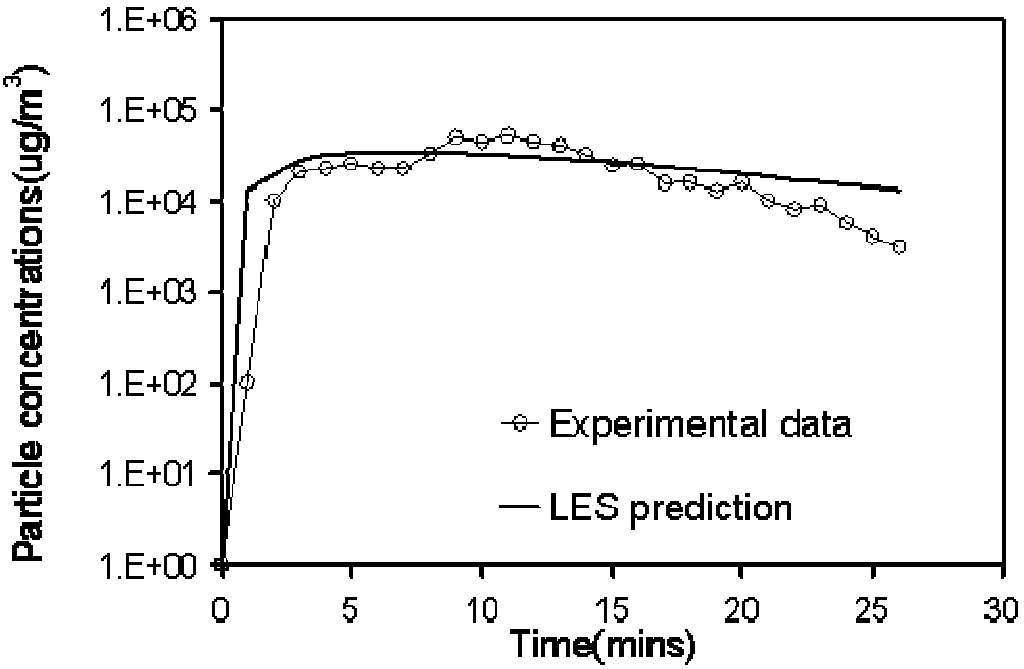


(b)

**Figure 5.16** The predicted and measured zone-averaged particle concentration decay ACH=9.216 1/H (a) zone 1 and (b) zone 2. (Particles depositing only on room floor)

The process of particles impacting on walls is taken into consideration by a particle-wall impact model. When reaching a wall surface, a contaminant particle either deposits or bounces depending on the presumed particle-wall impact type – the particle is "trapped" or

"reflected" respectively. It has been known that several physical parameters govern the particle-wall interaction process. Among these parameters are the electric force, molecular force, surface characteristics and roughness, particle incident velocity, diameter and shape of the particle as well as its material properties (Li et al., 2003 and Memarzadeh and Jiang, 2000). However, only two simple indoor particle-wall impact models for Lagrangian particle tracking model are currently used in literature: (i) particle bouncing from the wall, (ii) particle depositing on the surface (Memarzadeh and Jiang, 2000). According to the experimental investigations of Miguel et al. (2005), the indoor particle deposition is particularly significant for the floor surface, while the deposition on vertical and ceiling surfaces becomes important only when these surfaces are electrically charged. Herein, particles are assumed to deposit on the room's floor and bounce off other walls and ceilings.

For the case of particle bouncing, the normal and tangential restitution coefficients at wall boundaries, defining the amount of momentum in the directions normal and parallel to the wall that is retained by the particle after collision with the wall boundary, are determined as $e_n = -\frac{u_{rn}^p}{u_{in}^p}$ and $e_t = \frac{u_{rt}^p}{u_{it}^p}$ respectively. Where the subscripts *i* and *r* denote the incident and rebound components while *n* and *t* represent the normal and tangential directions respectively. Since the values regarding $e_n$ and $e_t$ are neither available in the experiment (Lu et al., 1996) nor in other literature, both $e_n$ and $e_t$ are assumed to be 0.9 to account for the restored kinetic energy of the particle after impact.

Figure 5.15(a) and 5.15(b) present the simulated and measured zone-averaged particle concentration decay in zone 1 and zone 2, respectively, for the case of 10.26 ACH. Here, the zone-averaged particle concentration *C* can be expressed as:

**Error! Objects cannot be created from editing field codes.** (5.1)

In zone 1, the RNG LES model predicts marginally lower contaminant particle concentration than the experimental data from t = 3 minutes to t = 15 minutes. Nevertheless, from the t = 15 minutes to t = 26 minutes, good agreement is subsequently achieved. After the 26$^{th}$ minute, the LES gives marginally higher concentration. In zone 2,

the LES model prediction is lower than the experimental data from the 2nd minute to 7th minute but thereafter good agreement is attained. Similar results for 9.26 ACH are also found in Figure 5.16(a) and 5.16(b). Here, lower prediction of particle concentration for zone 1 is obtained from t = 4 minutes to t = 10 minutes and a higher concentration is predicted after the 14th minute. Comparing to the experimental data, the RNG LES provides a higher concentration in zone 2 from the 9th minute to the 14th minute and a lower concentration after 14th minute. Overall, the RNG LES model combining with the Lagrangian model provides reasonable prediction of the zone-averaged contaminant particle concentration decay.

Several factors that may attribute to the marginal discrepancies between the predicted and measured particle concentration decay have been determined. Firstly, as shown in the numerical study of room 1, there is discrepancy between the predicted and measured airflow. This discrepancy could have an impact to the particle phase prediction. Secondly, the particles impacting a particular wall surface are assumed to be either "trapped" at the wall surface or "reflected" from the domain wall. These assumptions are not the case in real flows. It has been shown that the premise where particles are "reflected" occur only if the kinetic energy of a particle is greater than a critical threshold (Li and Ahmadi, 1993). Also, the normal and tangential coefficients of restitutions that should be determined experimentally are generally not given in the experiment (Lu et al., 1996). The influence of particle-wall impact model on the particle concentration prediction is investigated here. In the case of 10.26 ACH, the predicted concentration decays with three different assumptions of particle-wall interaction are compared. For the first assumption, particles are assumed to stick when reaching the room floor and to bounce when reaching other walls. The second set of assumptions is that particles bounce on all surfaces including the room floor. For the third assumption, particles are trapped on all surfaces.

Figure 5.17(a) and 5.17(b) show the comparison of the predicted particle concentration decay with these three assumptions for the case of 10.26 ACH. In zone 1, the simulated concentration of the second assumption, i.e. particles bouncing on all surfaces, is higher than the measured data after t = 10 minutes. For the assumption that the particles deposit on all surfaces, it is clearly seen that the predicted particle concentrations in zone 1 and zone 2 are significantly lower than other predictions and the experimental data. The above

comparisons show that the particle-wall impact model has an effect on the concentration prediction of Lagrangian particle-tracking model.

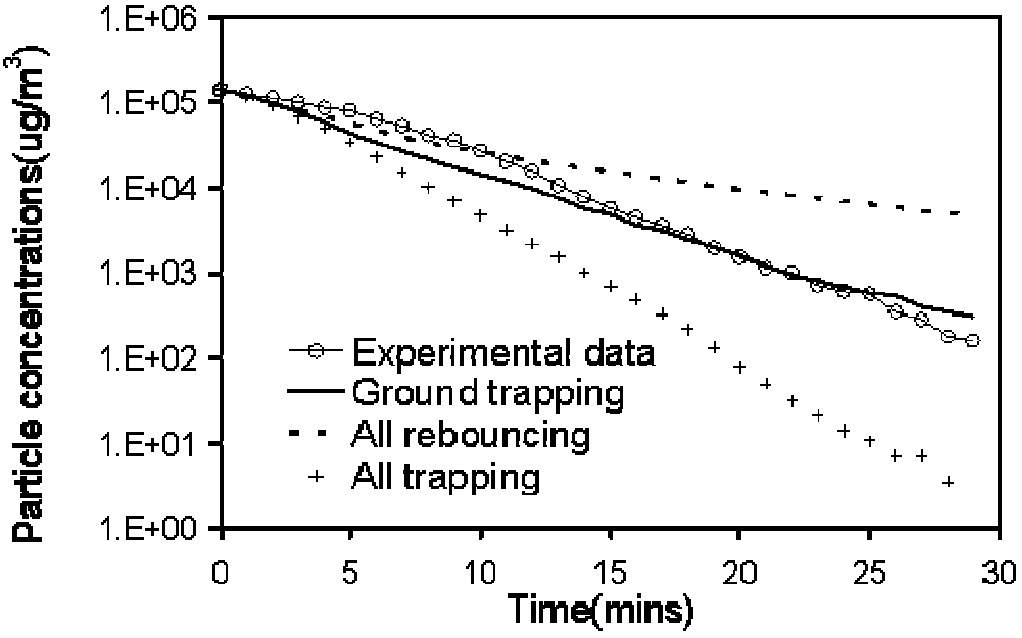


(a)

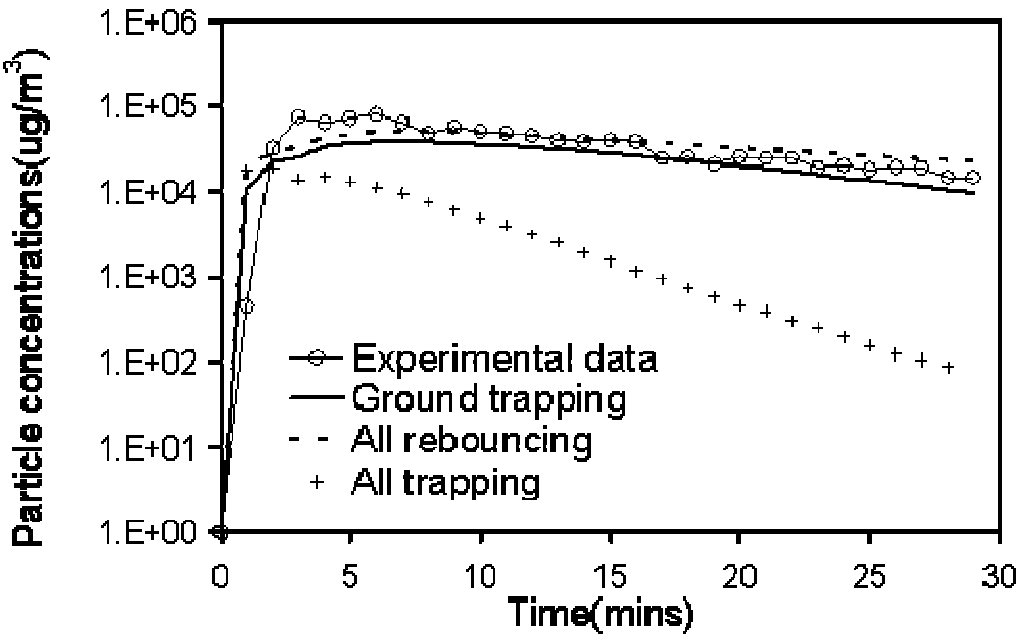


(a)

**Figure 5.17** The comparison of zone-averaged particle concentration decay with three assumptions ACH=10.26 (a) zone 1 and (b) zone 2.

Considerable investigations have been performed to study the indoor particle deposition experimentally, analytically and numerically (Miguel et al., 2005; Abadie et al., 2001; Lai, 2001). In these studies, the particle deposition is expressed in terms of the deposition velocity $v_d$ that is defined as:

$$v_d = \frac{J}{C_\infty} \tag{5.2}$$

where $J$ denotes the particle mass flux to the wall ( mass per unit area per unit time) and $C_\infty$ is a characteristic airborne particle concentration (mass per unit volume). This normalized flux has units of length per time that are the same as the units of velocity, though it represents a normalized transfer rate of the particles to the surface, rather than an averaged velocity of the particles moving toward the surface (Pesava et al., 1999). This approach of deposition velocity treats the particle deposition in a 'macroscopic' or 'statistical' way so that it can be implemented into the zonal model and two-fluid CFD model (Eulerian-Eulerian model) directly. For Lagrangian particle-tracking model, a 'microscopic' approach requires the deposition information for individual particles. The method of particle deposition velocity cannot therefore be applied to the Lagrangian model directly. At this juncture, no particle-wall impact model has been able to accurately predict the indoor contaminant particle concentration. A concerted effort is thus required to develop a more realistic particle-wall impact model to improve the Lagrangian prediction.

The particle concentration distributions in the room after an elapsed time of 5 minutes, 10 minutes and 15 minutes are illustrated in Figure 5.18 (a), (b) and (c), respectively. At t = 5 minutes, the higher particle concentration is found in zone 1, while higher concentrations are seen in zone 2 at t =10 and 15 minutes. It is notable that the particle concentration decay in zone 1 is faster than in zone 2, which is also showed in Figure 5.15 and Figure 5.16.

## 5.5 Summary

Through the numerical studies of the indoor airflows and contaminant particle concentration, the following observations are obtained:

- All the three turbulence models - standard $k$-ε, RNG $k$-ε and RNG-based LES models – provide good prediction of the air phase velocity; the RNG-based LES model prediction provides the best agreement with the measurements; the RNG $k$-ε gives better performance than standard $k$-ε model in velocity prediction.
- The RNG-based LES model is able to provide the instantaneous information such as the instantaneous air velocity and turbulence that is required for the evaluation and design of the ventilation system.
- The RNG-based LES model provides time-dependant LRN turbulence information to the particle phase, which results in more realistic particle dispersion and distribution than the conventional two-equation $k$-$\varepsilon$ models.
- As the experimental approach to access indoor contaminant particle concentration can be rather expensive and unable to provide the required detailed information, the LES prediction can be effectively employed to assess the performance of $k$-$\varepsilon$ models that are commonly applied in many building simulation investigations.
- The particle-wall impact model has a considerable effect on the particle concentration prediction.
- The numerical studies show that the two particle-wall impact models in literature (Memarzadeh and Jiang, 2000) either assuming particle bouncing from all the surfaces or assuming particle depositing on all the surfaces, are not adequate to accurately predict the indoor particle deposition for the Lagrangian particle tracking model.
- The predicted particle concentration decay is in acceptable agreement the experimental data (Lu et al., 1996) when the particles are assume to deposit on the floor and to rebound from other surfaces.
- Further theoretical and experimental studies are required to develop more realistic particle-wall impact models in order to improve the indoor particle prediction.

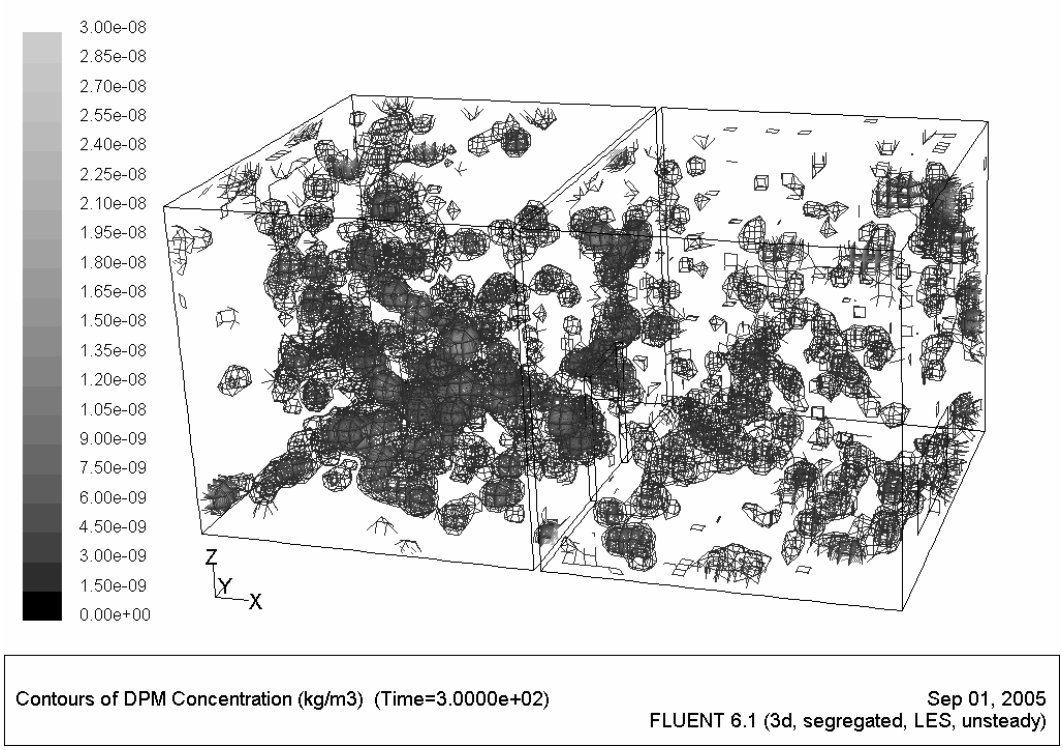
3.00e-08
2.85e-08
2.70e-08
2.55e-08
2.40e-08
2.25e-08
2.10e-08
1.95e-08
1.80e-08
1.65e-08
1.50e-08
1.35e-08
1.20e-08
1.05e-08
9.00e-09
7.50e-09
6.00e-09
4.50e-09
3.00e-09
1.50e-09
0.00e+00
Z
Y
X
Contours of DPM Concentration (kg/m3) (Time=3.0000e+02)
Sep 01, 2005
FLUENT 6.1 (3d, segregated, LES, unsteady)

(a)

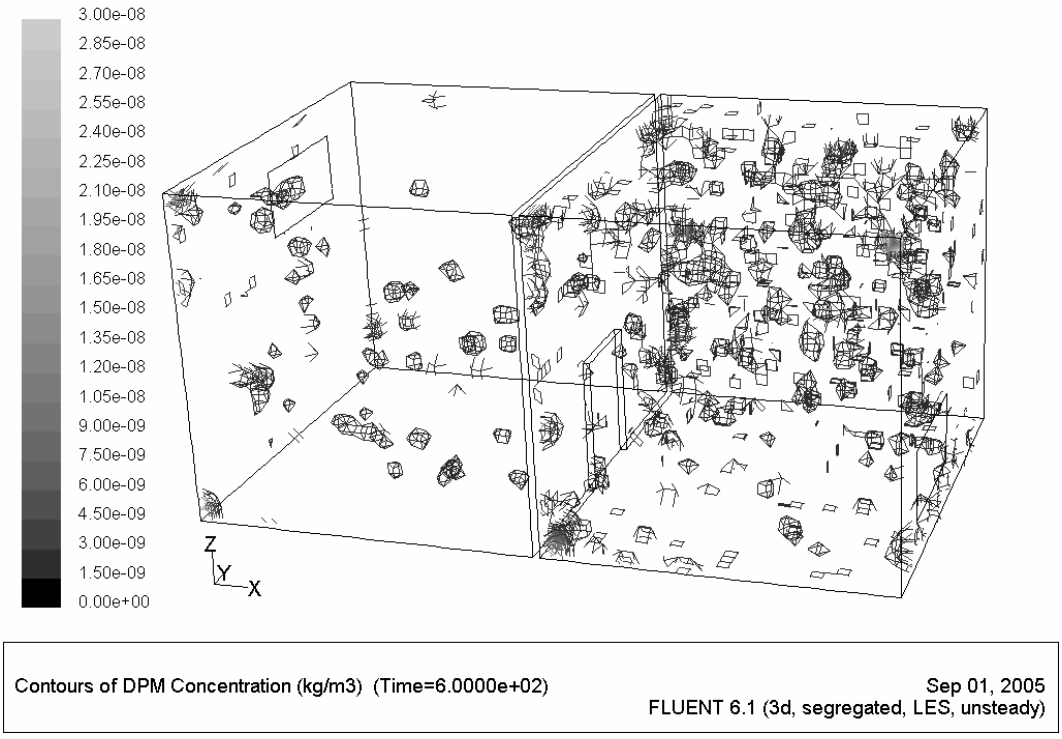
3.00e-08
2.85e-08
2.70e-08
2.55e-08
2.40e-08
2.25e-08
2.10e-08
1.95e-08
1.80e-08
1.65e-08
1.50e-08
1.35e-08
1.20e-08
1.05e-08
9.00e-09
7.50e-09
6.00e-09
4.50e-09
3.00e-09
1.50e-09
0.00e+00
Z
Y
X
Contours of DPM Concentration (kg/m3) (Time=6.0000e+02)
Sep 01, 2005
FLUENT 6.1 (3d, segregated, LES, unsteady)

(b)

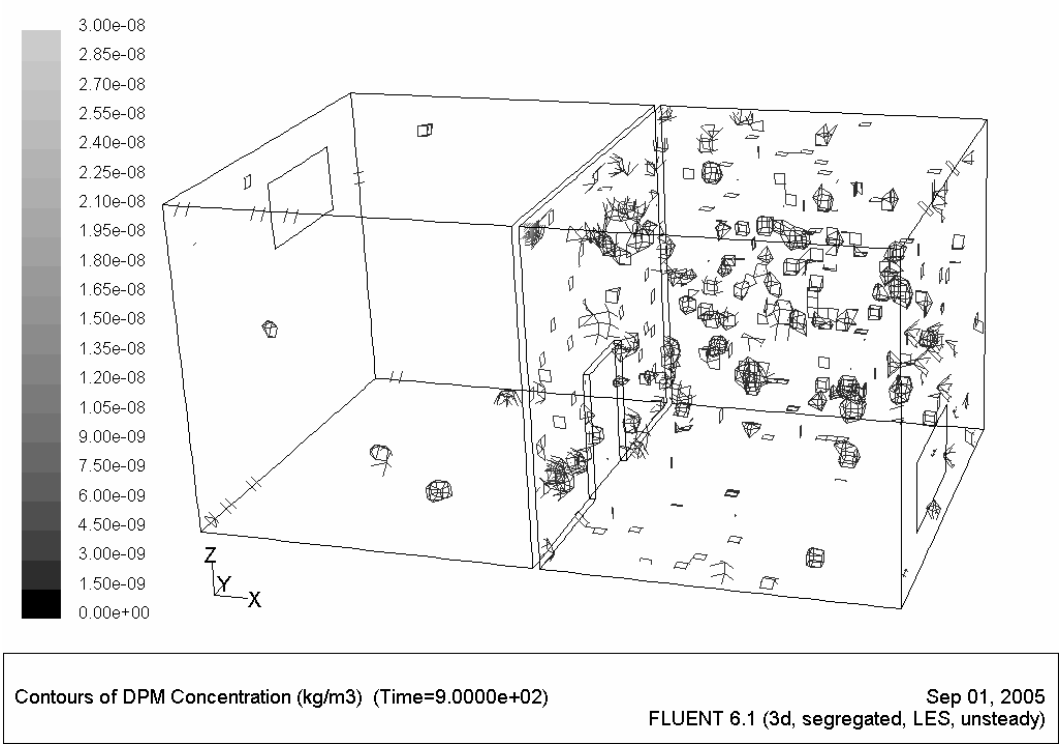


(c)

**Figure 5.18** The contaminant particle concentration distribution in room 2 after an elapsed time of (a) 5 minutes, (b) 10 minutes and (c) 15 minutes.